Full-Wave High-Order FEM Model for Lossy Anisotropic Waveguides

Patrizia Savi, *Member, IEEE*, Ioan-Ludovic Gheorma, and Roberto D. Graglia, *Fellow, IEEE*

***Abstract*—Anisotropic lossy waveguides are analyzed by applying the finite-element method with higher order interpolatory vector elements. The problem is formulated in terms of the electric field only. The transverse vector component of the electric field is numerically represented by higher order curl-conforming interpolatory vector functions, whereas the longitudinal component of the field is represented by higher order scalar basis functions. Due to the better interpolatory capabilities of the expansion functions, the metallic and material losses are modeled with a higher precision with respect to that provided by the other available numerical models. Furthermore, the use of higher order elements permits the correct modeling of the discontinuity of the normal field component at the interfaces between different materials.**

***Index Terms*—Finite-element method, guided-mode analysis, higher order basis functions.**

I. Introduction

VERY accurate and flexible computer-aided analysis and design techniques are required to deal with the increasing complexity of modern microwave and optical waveguide devices. For example, monolithic integrated circuits and devices often have lossy thick electrodes on substrates that exhibits dielectric and/or magnetic anisotropies and losses. To optimize performances, one must be able to correctly predict, during the design phase, the dependence on the fabrication parameters of the propagation characteristics and field distributions of these waveguide devices.

Among the most suitable methods [the mode-matching technique, method of lines, spectral-domain approach, integral-equation method, finite-difference method, and finite-element method (FEM)] to keep into account conductor and dielectric losses, anisotropies of both electric and magnetic kind, the FEM is probably the most generally applicable and the most versatile. For this reason, the literature devoted to FEM for microwave and optical waveguides is very wide and dates back to the early 1970s of the past century; in this connection, an extensive list of references is available in [1].

Different FEM formulations to deal with waveguide problems have been proposed in the literature. A number of these are reviewed and compared from several points of view in [2] by classifying the principal FEM formulations also according to the number of field components used, i.e., two or three. The reduction from three field components to two always results in the loss of either sparsity or symmetry in the matrix equation [2]. In order to deal with general lossy anisotropic media in terms of sparse FEM matrices, it is necessary to keep three field components; early examples of lossless waveguide problems numerically solved by applying a three field components formulation are given in [3], [4].

A good review of several different ways to avoid spurious solutions in the FEM analysis of waveguide problems is given in [5], while presenting a two-component FEM approach to study inhomogeneous lossy waveguides with dielectric gyrotropic materials. The best remedy to avoid the spurious FEM solutions due to improper modeling of the null space of the curl operator (see [6]) is to use *curl-conforming* vector bases or tangential elements [3].

In order to improve the convergence of the numerical solution, high-order vector elements are often used. For example, a dramatic improvement in the convergence of the numerical results for optical waveguides has been observed in [7] just by use of first-order vector elements. Although [7] associates some degrees of freedom to values of the transverse field at element corner nodes, it nevertheless develops a numerical expansion of a three-component vector unknown, similar to the one presented here and to the one used in [8] and [9] to deal with lossy waveguides in terms of zeroth-order vector elements.

In general, high-order elements either belong to a hierarchical family or they can get interpolatory forms. A family is hierarchical if all the basis functions of the pth-order set are a subset of the basis functions forming the set of order $(p+1)$; for this reason, the hierarchical (vector) set of order $(p+1)$ cannot be made interpolatory at the same time.

In general, when interpolatory vector elements are used, the order p of the basis functions is the same (p is kept constant) on the whole computational domain. High-order *interpolatory* forms of curl-conforming vector bases have been systematically constructed for all the commonly used elements: triangular and quadrilateral elements for the two-dimensional (2-D) cases, tetrahedral, brick, pentahedral and pyramidal elements for the three-dimensional (3-D) case [10]–[12].

Hierarchical elements are usually employed when one has the need to iteratively increase, on a given mesh, the order of the used basis functions in some part of the computational domain [13]–[15]. In fact, large complex problems can be approached by iterative FEM schemes where, at each iteration step, one improves the solution only in those regions of the computational domain where the numerical error of the previous step was

Manuscript received April 7, 2000; revised March 13, 2001. This work was supported in part by the Italian National Research Council under Grant 98.00831.CT07 and Grant 99.00113.48, by the Italian Ministry of University and Scientific Research, and by the Microwave Engineering Center for Space Applications, Italy.

P. Savi and R. D. Graglia are with the Dipartimento di Elettronica, Politecnico di Torino, 10129 Turin, Italy.

I.-L. Gheorma is with the Microelectronic Sciences Laboratory, Columbia University, New York, NY 10027 USA.

Publisher Item Identifier S 0018-9480(02)01162-6.

found higher than a threshold. These improvements are obtained either by using a denser mesh, in the required regions, without changing the order of the used elements (h adaption) or by locally increasing the order of the elements without redefining the mesh (p adaption). Indeed, to be effective, p-adaptive schemes require the use of *hierarchical* vector basis functions, whereas h-adaptive schemes can be implemented by using interpolatory vector elements.

The interpolatory vector bases used in this paper were generated by multiplying the zeroth-order basis functions times a complete set of *interpolatory* polynomials, with redundancy elimination, as described in [10]. Conversely, hierarchical basis functions can be obtained by multiplying the zeroth-order vector functions times a hierarchical family of (scalar) polynomials [14].

In this paper, we provide a general three-component FEM formulation of the lossy anisotropic waveguide problem. The ensuing FEM discretization is obtained by using interpolatory functions of arbitrarily high order on triangular elements. The superiority of the higher order model is assessed by studying several examples. In particular, by considering an inhomogeneously filled waveguide, it is shown that the use of high-order elements permits the correct modeling of the discontinuity of the normal field component at the interfaces between different materials. This method is then applied to study shielded waveguiding structures such as striplines of the most general type: with metallic regions of finite thickness and finite conductivity, and with lossy anisotropic nonhomogeneous substrates. For thick metal strips of finite conductivity, the current density distribution cannot be approximated by a surface current density. In this case, the metallic regions of finite conductivity are discretized and the field is computed therein. This allows for a very precise evaluation of the lossy phenomena.

II. Formulation

The full-wave model of a uniform anisotropic waveguide along the z-axis is obtained from the frequency-domain Helmholtz's vector equation

$$\boldsymbol{\nabla}\times\left[\underline{\underline{\boldsymbol{\mu}}}_r^{-1}\cdot(\boldsymbol{\nabla}\times\boldsymbol{E})\right]-k_0^2\,\underline{\underline{\boldsymbol{\epsilon}}}_r\cdot\boldsymbol{E}=0 \tag{1}$$

by assuming and suppressing a longitudinal-dependence factor $\exp(-jk_zz)$ for the total electric field $\boldsymbol{E}=(\boldsymbol{E}_t+E_z\hat{\boldsymbol{z}})$, with $\boldsymbol{\nabla}=\boldsymbol{\nabla}_t-jk_z\hat{\boldsymbol{z}}$ and $(\boldsymbol{\nabla}_t\times\boldsymbol{E}_t)_z=\hat{\boldsymbol{z}}\cdot(\boldsymbol{\nabla}_t\times\boldsymbol{E}_t)$. In (1), $k_0=\omega\sqrt{\epsilon_0\mu_0}$ is the free-space wavenumber and μ_0 and ϵ_0 are the free-space permeability and permittivity, respectively; whereas $\underline{\underline{\boldsymbol{\epsilon}}}_r$ and $\underline{\underline{\boldsymbol{\mu}}}_r$ are the relative permittivity and permeability tensors, respectively.

In case of shielded waveguides, the boundary γ of the waveguide cross section S is made of conducting material; conversely, for unshielded waveguides, γ is a fictitious geometrical boundary introduced to limit the domain of the problem. By weighting (1) with a testing function $\boldsymbol{T}\exp(-jk_zz)=(\boldsymbol{T}_t+T_z\hat{\boldsymbol{z}})\exp(-jk_zz)$ on the domain S, application of the divergence theorem yields the integral residual

$$\begin{aligned}\iint_S\Big[&(\boldsymbol{\nabla}_t\times\boldsymbol{T}_t)_z\mu_{zz}^{\mathrm{inv}}(\boldsymbol{\nabla}_t\times\boldsymbol{E}_t)_z\\&+(\boldsymbol{\nabla}_tT_z+jk_z\boldsymbol{T}_t)\cdot\underline{\underline{\boldsymbol{\nu}}}_t\cdot(\boldsymbol{\nabla}_tE_z+jk_z\boldsymbol{E}_t)\\&+(\boldsymbol{\nabla}_tT_z+jk_z\boldsymbol{T}_t)\cdot\boldsymbol{\upsilon}_t(\boldsymbol{\nabla}_t\times\boldsymbol{E}_t)_z\\&+(\boldsymbol{\nabla}_t\times\boldsymbol{T}_t)_z\tilde{\boldsymbol{\upsilon}}_t\cdot(\boldsymbol{\nabla}_tE_z+jk_z\boldsymbol{E}_t)\\&-k_0^2(\boldsymbol{T}_t\cdot\underline{\underline{\boldsymbol{\epsilon}}}_t\cdot\boldsymbol{E}_t+T_z\epsilon_{zz}E_z)\Big]\,dS\\+\int_\gamma&\left[\boldsymbol{T}\cdot\hat{\boldsymbol{n}}\times\left(\underline{\underline{\boldsymbol{\mu}}}_r^{-1}\cdot\boldsymbol{\nabla}\times\boldsymbol{E}\right)\right]d\gamma=0\end{aligned} \tag{2}$$

with

$$\mu_{zz}^{\mathrm{inv}}=\hat{\boldsymbol{z}}\cdot\underline{\underline{\boldsymbol{\mu}}}_r^{-1}\cdot\hat{\boldsymbol{z}} \tag{3}$$

$$\underline{\underline{\boldsymbol{\nu}}}_t=-\hat{\boldsymbol{z}}\times\underline{\underline{\boldsymbol{\mu}}}_r^{-1}\times\hat{\boldsymbol{z}} \tag{4}$$

$$\boldsymbol{\upsilon}_t=\hat{\boldsymbol{z}}\times\underline{\underline{\boldsymbol{\mu}}}_r^{-1}\cdot\hat{\boldsymbol{z}} \tag{5}$$

$$\tilde{\boldsymbol{\upsilon}}_t=-\hat{\boldsymbol{z}}\cdot\underline{\underline{\boldsymbol{\mu}}}_r^{-1}\times\hat{\boldsymbol{z}} \tag{6}$$

and where $\underline{\underline{\boldsymbol{\epsilon}}}_t(=-\underline{\underline{\boldsymbol{\epsilon}}}_r\times\hat{\boldsymbol{z}}\times\hat{\boldsymbol{z}})$ is the transverse component of $\underline{\underline{\boldsymbol{\epsilon}}}_r$, whereas $\epsilon_{zz}=\hat{\boldsymbol{z}}\cdot\underline{\underline{\boldsymbol{\epsilon}}}_r\cdot\hat{\boldsymbol{z}}$. Equation (2) considerably simplifies for gyrotropic tensor $\underline{\underline{\boldsymbol{\mu}}}_r$ with a principal axis along the waveguide axis z since the transverse vectors $\boldsymbol{\upsilon}_t$ and $\tilde{\boldsymbol{\upsilon}}_t$, defined in (5) and (6), vanish in this case.

Evaluation of the γ-contour integral in (2) is not required to deal with shielded waveguiding structures bounded by perfectly conducting walls. In fact, the boundary condition on a perfect magnetic wall implies $\hat{\boldsymbol{n}}\times(\underline{\underline{\boldsymbol{\mu}}}_r^{-1}\cdot\boldsymbol{\nabla}\times\boldsymbol{E})=0$, whereas on a perfect electric wall, the vanishing of the tangent electric field is readily imposed by appropriate choice of the functions used to expand the vector field $\boldsymbol{E}$. In this paper, we deal with shielded waveguides only.

By use of a Galerkin form of the finite-element method, (2) is discretized by following a rather standard procedure similar to that given in [3]. This yields a complex generalized eigenvalue problem solved by use of an iterative method. The waveguide modal field distributions are obtained as the eigenvectors of the generalized problem.

In our numerical approach, the transverse vector component of the electric field $\boldsymbol{E}_t$ is modeled by high-order curl-conforming elements, whereas the longitudinal component E_z is modeled by high-order nodal elements. Use of these elements ensures the continuity of tangential field components at element interfaces, eliminates spurious modes and facilitates the enforcement of the boundary conditions. A triangular mesh is used to discretize the waveguide cross section S, and the higher order interpolatory forms of the curl-conforming vector bases we use are those given in [10].

It is of paramount importance that the scalar basis functions used to model the longitudinal field E_z and its gradient have the same order of those used to represent $\boldsymbol{E}_t$ and its curl. Since (2) requires the computation of $\boldsymbol{\nabla}_tE_z$, the interpolatory scalar expansion functions must be linear at order $p=0$ and have to ensure the continuity of the longitudinal field component at element interfaces. Thus, three scalar functions are required for zeroth-order completeness on a triangle. For higher order scheme,

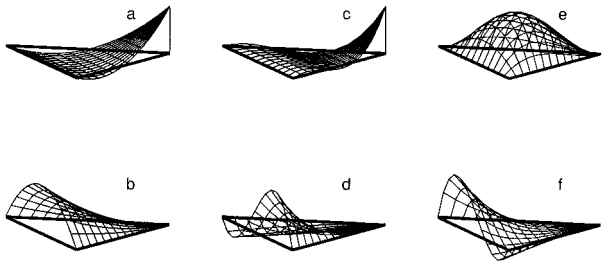

Fig. 1. Scalar basis functions for complete first- and second-order representation of the longitudinal component E_z. (a), (b) For $p = 1$. (c)–(f) For $p = 2$.

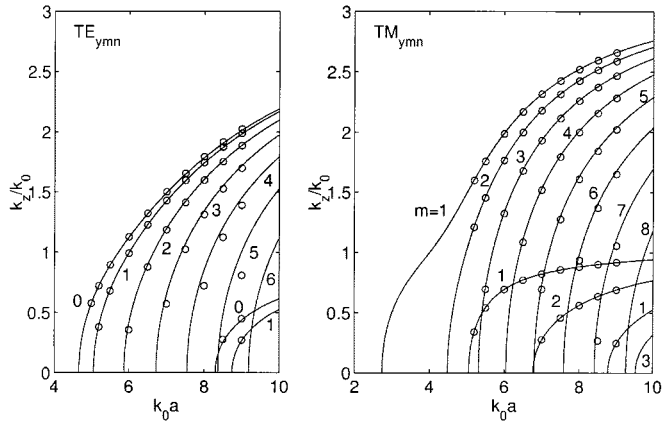

Fig. 2. Dispersion diagram for a rectangular waveguide ($a = 2b$) containing a thin dielectric slab ($\epsilon_r = 10$) of thickness $t = 0.2b$. TE_{ym} results are given on the left-hand side, while TM_{ym} results are shown on the right-hand side. Analytical results are reported by solid lines; the circles show the FEM results obtained with $p = 1$.

the order of the scalar expansion functions must increase. That is to say, if the transverse vector component of the electric field $\boldsymbol{E}_t$ is represented by curl-conforming functions of order p [10], the longitudinal expansion functions must form a complete polynomial set of order $p + 1$ on a triangle. In order to reach pth order completeness, the total number of nodal functions per triangle is $(p+2)(p+3)/2$. High-order scalar (Lagrange) elements are easily defined on a triangle [17]; the interpolation points of these functions are arranged as in the Pascal triangle. Triangular nodal functions for $p = 1$ and $p = 2$ are shown in Fig. 1. Three corner [see Fig. 1(a)] plus three midside node functions [see Fig. 1(b)] are required for $p = 1$. For $p = 2$, one has three corner node functions [see Fig. 1(c)], six midside node functions [see Fig. 1(d) and (f)], and one internal node function [see Fig. 1(e)].

III. Superiority of the Higher Order Model

As a critical test case, we first consider a rectangular waveguide of size a along the x-axis and $b = a/2$ along the y-axis. The waveguide is dielectric filled between $y = 0$ and $y = 0.2b$ with a material of relative permittivity $\epsilon_r = 10$. Fig. 2 reports the dispersion curves of this waveguide obtained by applying the transverse resonance technique [18]. Results for modes transverse electric with respect to y (TE_{y_m} modes) are reported on the left-hand side, whereas results for modes transverse magnetic with respect to y (TM_{y_m}) are given on the right-hand side. The modal index m refers to the x component $k_x = m\pi/a$

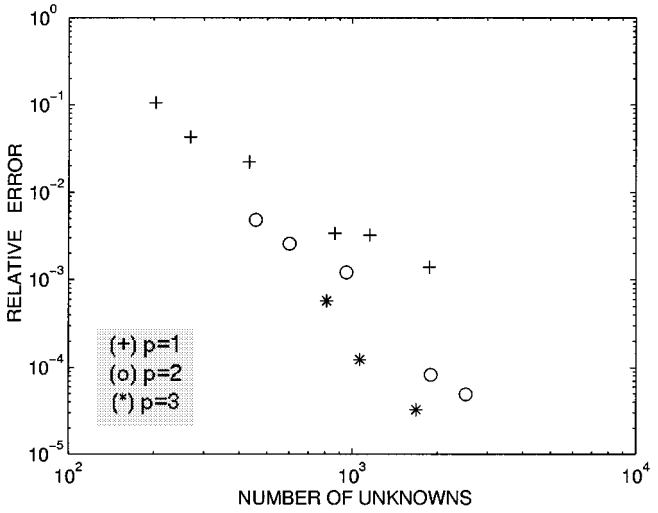

Fig. 3. Relative error for the first 11 modes at $k_0a = 7$ and $p = 1, 2, 3$ for the inhomogeneously filled rectangular waveguide of Fig. 2.

of the transverse wavenumber. The circles show the FEM results obtained with $p = 1$ (280 elements, 163 corner nodes, and 1873 unknowns); these agree very well with the analytic results up to $k_oa \sim 8$. Results relative to higher order elements are not reported; in fact, e.g., the results obtained by using a rather coarse mesh (44 elements, 33 corner nodes) with $p = 3$ (1065 unknowns), are undistinguishable from the analytic results.

The relative errors on k_z for the first 11 modes at $k_0a = 7$ are shown in Fig. 3 versus the number of unknowns (internal degrees of freedom). Results for $p = 0$ are not shown because only ten modes are clearly distinguishable with $p = 0$ at $k_0a = 7$ in the range considered (number of unknowns). These results show the faster convergence achievable by using higher order elements.

Notice also that only higher order elements permit to correctly model the discontinuity of the normal field components at interfaces between different materials. For example, Fig. 4 shows the ratio E_{y_a}/E_{y_d} of the normal components of the electric field along the air/dielectric interface at $y = 0.2b$ for the fundamental mode of the previous inhomogeneously filled rectangular waveguide evaluated with $p = 0, 1, 2, 3$. These results were obtained by using approximately the same number of unknowns (≈1800). The divergent behavior at the boundaries $x = 0$ and $x = a$ is due to the vanishing of the y-component of the electric field on the lateral metal boundaries. Note that these results approach the correct value of $E_{y_a}/E_{y_d} = 10$ at the interface only for $p \geq 2$. Incorrect results are always obtained with $p = 0$, even when a much larger number of unknowns is used. This evidence is easily explained by noticing that the correct jump of the field component, normal to the triangle edges, can be modeled only if a sufficient number of interior degrees of freedom is available. For $p = 1$, each triangular curl-conforming element contributes with only two interior degrees of freedom [10], whereas the element has three edges. For $p = 2$, there are six (transverse) interior degrees of freedom per triangle and, hence, there is the possibility to model the normal field discontinuity (or continuity) at each element edge. Furthermore, notice that the effect of the mesh discretization is quite evident

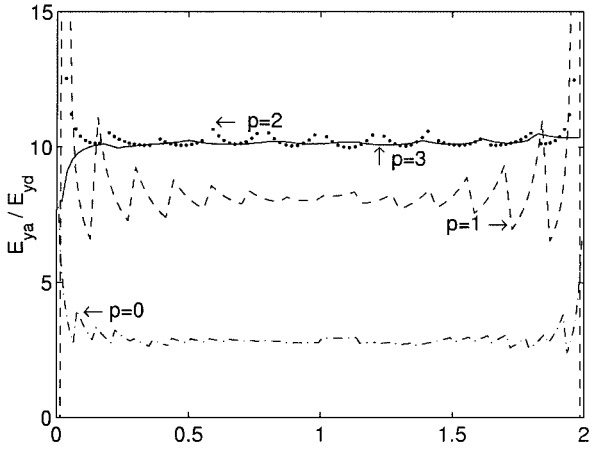

Fig. 4. Normal electric field discontinuity at the interface dielectric–air for the inhomogeneously filled rectangular waveguide. Number of edges located on the interface: 28 for $p = 0$, 14 for $p = 1$, ten for $p = 2$, and eight for $p = 3$. Total number of unknowns: 2153 for $p = 0$, 1873 for $p = 1$, 1897 for $p = 2$, and 1681 for $p = 3$.

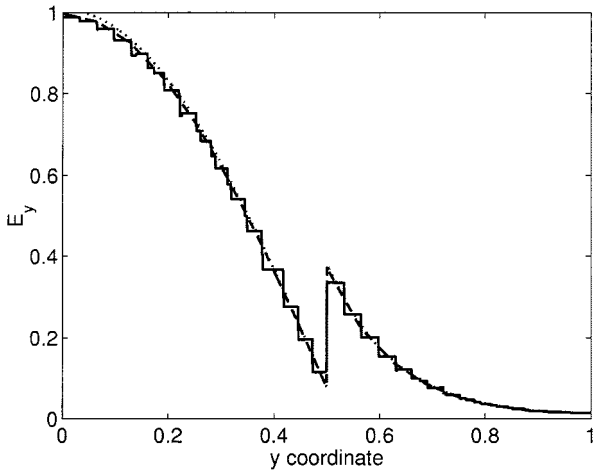

Fig. 5. Normal electric field component along vertical line for an half-filled rectangular waveguide ($a/b = 2$, $\epsilon_r = 5$). Total number of unknowns: 5697 for $p = 0$ (solid line), 4969 for $p = 1$ (dashed line), and 2635 for $p = 2$ (dotted line).

for zeroth-, first-, and second-order elements, while it almost disappears when third-order elements are used.

To clarify the modeling of the field continuity from element to element, let us consider again a rectangular waveguide ($a/b = 2$) half filled with a material of relative permittivity $\epsilon_r = 5$ for $0 < y < b/2$. Fig. 5 shows the y-component of the electric field for the fundamental mode along a vertical straight line drawn at $x \simeq a/2$. The results for $p = 0, 1$, and 2 were obtained with 5697, 4969, 2635 unknowns, respectively. The correct jump of the vertical field component at $y = b/2$ is five. Numerically, we have found 4.8 for $p = 0$, 4.83 for $p = 1$, and 4.87 for $p = 2$.

In the case of $p = 0$, for the y-field component, a staircase approximation is obtained, as expected, since zeroth-order functions can correctly model only constant field within each elements. For $p = 1$, the approximation is piecewise linear, for $p = 2$, second-order approximation is obtained, and so on.

The error in modeling the normal discontinuity (or continuity) of the field component at element edges is, in general, of concern only for edges located on a boundary separating materials with different electromagnetic parameters. In fact, the direction normal to a given separation boundary is also normal to all the edges modeling this boundary. Conversely, an arbitrary line drawn in a homogeneous region will cut element edges at different angles, not always at 90°. In this case, the continuity of the field component tangent to the line will be satisfied everywhere at the proper order in the homogeneous region, with the exception of those points of the given line belonging to more than one element. At these points, the error will be greater if the line happens to be orthogonal to an element edge.

To show that high-order elements can be effectively used on coarse meshes, in Fig. 6 some results relative to an image line, consisting of a rectangular waveguide ($a = 1.3$ mm, $b = 1.6$ mm) with a rutile anisotropic insert (permittivity $\epsilon_{rx} = 170$, $\epsilon_{ry} = \epsilon_{rz} = 85$) of rectangular cross section ($a' = 0.55$ mm $b' = 0.82$ mm) are shown. The two meshes used to study this structure are shown in the inset of Fig. 6. The coarse mesh has 24 triangles and 19 corner nodes and yields 37, 145, 325, 577,

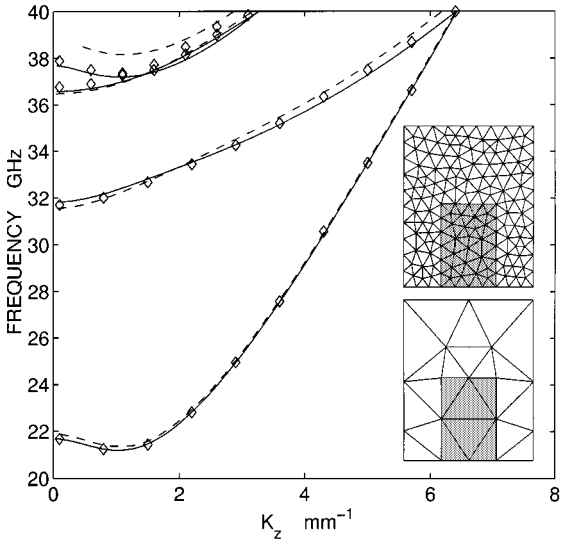

Fig. 6. Dispersion diagram for the image line described in the text. Solid line: results for $p = 2$ (325 unknowns), coarse mesh. Dash line: results for $p = 0$ (544 unknowns), dense mesh. Diamonds: results taken from [19].

and 901 unknowns at $p = 0, 1, 2, 3$, and 4, respectively. The dense mesh has 291 triangles and 166 corner nodes and yields 544 unknowns at $p = 0$, which is a number of unknowns comparable to the number one has by using $p = 3$ on the coarse mesh. The results obtained with the dense mesh for $p = 0$ (37 unknowns) are reported in Fig. 6 by dashed lines; solid-line results are relative to the coarse mesh with $p = 2$ (325 unknowns). Our results are compared with the mode expansion results of [19] obtained by using 200 modes; in [19], the convergence of the modal expansion results has been proven for the dominating mode only. Notice that this test case is also considered in [16, p. 210]. The results relative to the third and fourth mode provided by our dense mesh with $p = 0$ are of poor quality; convergence of our numerical results for $p = 2$ on the coarse mesh has been verified by comparison with the results obtained by using $p = 3$ and $p = 4$.

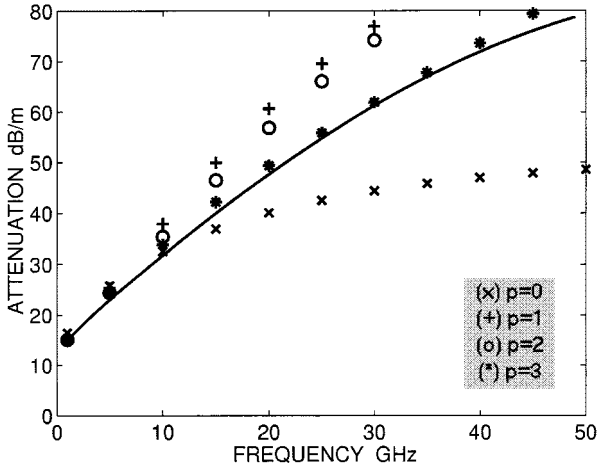

Fig. 7. Attenuation constant for the microstrip line described in the text. The solid line results are taken from [20].

IV. Results for Lossy Waveguides

High-order elements can be effectively used to model the complex behavior of electromagnetic fields in lossy metal regions having dimension of the same order of the skin depths of some frequency components. For example, let us consider a lossy microstrip line on a (lossless) GaAs substrate of height $h = 100$ μm and permittivity $\epsilon_r = 13$. The line parameters are: linewidth $W = 75$ μm, strip and ground plane thickness $t = 3$ μm, strip conductivity $\sigma = 4.1 \cdot 10^7$ S/m, ground-plane conductivity $\sigma = 5.8 \cdot 10^7$ S/m. This structure has been studied by enclosing it in a square perfectly conducting box of size 20 W. To numerically deal with such a structure, high-order quadrilateral elements are more convenient than triangular elements because of the presence of very thin rectangular regions (the strip and ground plane). Despite the fact that good models could be obtained by use of specialized preprocessor codes, to prove the effectiveness of high-order elements on a general triangular mesh, the geometry has been readily discretized with a triangular mesh by use of a commercially available code (PDETOOL–MATLAB).

The mesh we used consists of 420 triangles and 733 corner nodes, corresponding to ~14 000 unknowns for $p = 0$ and to roughly 960 000 unknowns for $p = 3$. In spite of these high figures relevant to the number of degrees of freedom, this mesh yields a questionable model for the electromagnetic field in the lossy ground plane and within the strip. In particular, the strip is coarsely modeled by only one layer of eight triangle doublets, which is to say, by 16 right-angled triangles in all. Each triangle within the strip is of poor quality since its orthogonal sides have very unequal length (3 and ~9 μm). Therefore, appropriate expansion functions able to accurately represent the field decay in the metal region are necessary to a reliable evaluation of the losses. It is rather evident that this is impossible just by using zeroth-order functions and only one layer of triangle doublets within the strip. In fact, the strip thickness t equals two skin depths ($t = 2\delta$) at $f \simeq 2.75$ GHz, whereas at 40 GHz, the strip skin depth is roughly $0.13t$ (δ is 0.39 μm). To get good results with $p = 0$, one needs to define at least three layers of triangle doublets in the ground plane and within the strip (with 132 triangles in the strip region).

In Fig. 7, the attenuation constant evaluated for $p = 0, 1, 2$, and 3 is compared with the result of [20], obtained by using 551 zeroth-order rectangular elements. The propagation constant results are not reported since they are always in excellent agreement with those of [20], independently from the chosen p value. As a matter of fact, from Fig. 7, one can appreciate the convergence of our results to the reference solution for increasing order p of the expansion functions.

The number of unknowns required to study this lossy microstip line can be reduced by using appropriate boundary conditions on artificial boundaries defined to reduce and close the mesh region. A more significant reduction in the number of unknowns is achievable by resorting to solution schemes that involve high-order functions only in the regions where these are needed (p adaption or, for example, as in [21]). These improvements are not discussed here since they are outside the point of this paper.

V. Conclusions

A higher order vector FEM code to study shielded waveguides with lossy anisotropic regions and with metallic regions of finite thickness and finite conductivity has been implemented. We have shown that higher order vector elements are essential to correctly model the normal discontinuity of the field at the interface between two different media, and to accurately model the conductor losses in roughly meshed metal regions of dimension of the same order of the skin depths of some frequency components.

References

[1] B. M. A. Rahman, F. A. Fernandez, and J. B. Davies, "Review of finite element methods for microwave and optical waveguides," *Proc. IEEE*, vol. 79, pp. 1442–1448, Oct. 1991.

[2] B. M. Dillon and J. P. Webb, "A comparison of formulations for the vector finite element analysis of waveguides," *IEEE Trans. Microwave Theory Tech.*, vol. 42, pp. 308–316, Feb. 1994.

[3] J.-F. Lee, D-K. Sun, and Z. J. Cendes, "Full-wave analysis of dielectric waveguides using tangential vector finite elements," *IEEE Trans. Microwave Theory Tech.*, vol. 39, pp. 1262–1271, Aug. 1991.

[4] M. Matsuhara, H. Yunoki, and A. Maruta, "Analysis of open-type waveguides by the vector finite element method," *IEEE Microwave Guided Wave Lett.*, vol. 1, pp. 376–378, Dec. 1991.

[5] Y. Lu and F. A. Fernandez, "An efficient finite element solution of inhomogeneous anisotropic and lossy dielectric waveguides," *IEEE Trans. Microwave Theory Tech.*, vol. 51, no. 6, pp. 1215–1223, June–July 1993.

[6] S. H. Wong and Z. J. Cendes, "Combined finite element-modal solution of three-dimensional eddy current problems," *IEEE Trans. Magn.*, vol. 24, pp. 2685–2687, Nov. 1988.

[7] M. Koshiba, S. Maruyama, and K. Hirayama, "A vector finite element method with the high-order mixed-interpolation-type triangular elements for optical waveguiding problems," *J. Lightwave Technol.*, vol. 12, pp. 495–501, Mar. 1994.

[8] J.-F. Lee, "Finite element analysis of lossy dielectric waveguides," *IEEE Trans. Microwave Theory Tech.*, vol. 42, pp. 1025–1031, June 1994.

[9] L. Valor and J. Zapata, "Efficient finite element analysis of waveguides with lossy inhomogeneous anisotropic materials characterized by arbitrary permittivity and permeability tensors," *IEEE Trans. Microwave Theory Tech.*, vol. 43, pp. 2452–2458, Oct. 1995.

[10] R. D. Graglia, D. R. Wilton, and A. F. Peterson, "Higher order interpolatory vector bases for computational electromagnetics," *IEEE Trans. Antennas Propagat.*, vol. 45, pp. 329–342, Mar. 1997.

[11] R. D. Graglia, D. R. Wilton, A. F. Peterson, and I.-L. Gheorma, "Higher order interpolatory vector bases on prism elements," *IEEE Trans. Antennas Propagt.*, vol. 46, pp. 442–450, Mar. 1998.
[12] R. D. Graglia and I.-L. Gheorma, "Higher order interpolatory vector bases on pyramidal elements," *IEEE Trans. Antennas Propagat.*, vol. 47, pp. 775–782, May 1999.
[13] L. S. Andersen and J. L. Volakis, "Hierarchical tangential vector finite elements for tetrahedra," *IEEE Microwave Guided Wave Lett.*, vol. 8, pp. 127–129, Mar. 1998.
[14] ——, "Development and application of a novel class of hierarchical tangential vector finite elements for electromagnetics," *IEEE Trans. Antennas Propagat.*, vol. 47, pp. 112–120, Jan. 1999.
[15] J. P. Webb, "Hierarchal vector basis functions of arbitrary order for triangular and tetrahedral finite elements," *IEEE Trans. Antennas Propagat.*, vol. 47, pp. 1244–1253, Aug. 1999.
[16] J. Jin, *The Finite Element Method in Electromagnetics*. New York: Wiley, 1993.
[17] P. P. Silvester and R. L. Ferrari, *Finite Elements for Electrical Engineers*. Cambridge, U.K.: Cambridge Univ. Press, 1990.
[18] R. F. Harrington, *Time–Harmonic Electromagnetic Fields*. New York: McGraw-Hill, 1961.
[19] J. I. H. Askne, E. L. Kollberg, and L. Pettersson, "Propagation in a waveguide partially filled with anisotropic dielectric material," *IEEE Trans. Microwave Theory Tech.*, vol. 30, pp. 795–799, May 1982.
[20] J. Tan and G. Pan, "A new edge element analysis of dispersive waveguides structures," *IEEE Trans. Microwave Theory Tech.*, vol. 43, pp. 2600–2607, Nov. 1995.
[21] R. S. Preissig and A. F. Peterson, "Application of p-refinement techniques to vector finite elements," in *URSI Nat. Radio Science Meeting Dig.*, 1998, p. 206.

Patrizia Savi (M'00) received the Electronic Engineering degree from the Politecnico di Torino, Turin, Italy in 1985.

In 1986, she was involved with the analysis and design of dielectric radomes at Alenia (Caselle Torinese). Since 1987, she has been a Researcher at the Centro Studi Propagazione e Antenne (CeSPA), Italian National Research Council (CNR), Politecnico di Torino. Since 1998, she has been a member of the Dipartimento di Elettronica, Politecnico di Torino, where she is currently an Associate Professor and teaches courses on electromagnetic-field theory. Her research interests are in the area of dielectric radomes, frequency-selective surfaces, radar cross section, waveguide discontinuities and microwave filters, and numerical techniques.

Ioan-Ludovic Gheorma received the M.S. degree (with honors) in electrical engineering from the Polytechnic University of Bucharest, Bucharest, Romania, in 1997, and is currently working toward the Ph.D. degree in electrical engineering at Columbia University, New York, NY. His doctoral dissertation concerns specialization microwave photonics.

His main research interest are photonic integrated circuits and computational electromagnetics.

Roberto D. Graglia (S'83–M'83–SM'90–F'98) was born in Turin, Italy, on July 6, 1955. He received the Laurea degree (*summa cum laude*) in electronic engineering from the Politecnico di Torino, Turin, Italy, in 1979, and the Ph.D. degree in electrical engineering and computer science from the University of Illinois at Chicago, in 1983.

From 1980 to 1981, he was a Research Engineer at the Centro Studi e Laboratori Telecomunicazioni (CSELT), Italy, where he conducted research on microstrip circuits. From 1981 to 1983, he was a Teaching and Research Assistant at the University of Illinois, Chicago. From 1985 to 1992, he was a Researcher with the Italian National Research Council. In 1991 and 1993, he was Associate Visiting Professor at the University of Illinois, Chicago. In 1992, he joined the Dipartimento di Elettronica, Politecnico di Torino, as an Associate Professor. He has been a Professor of electrical engineering in that department since 1999. His areas of interest comprise numerical methods for high- and low-frequency electromagnetics, theoretical and computational aspects of scattering and interactions with complex media, waveguides, antennas, electromagnetic compatibility, and low-frequency phenomena. He has organized and taught several short courses in those areas. Since 1997, he has been a member of the Editorial Board of *Electromagnetics*.

Dr. Graglia is a past associate editor of the IEEE TRANSACTIONS ON ANTENNAS AND PROPAGATION and past associate editor of the IEEE TRANSACTIONS ON ELECTROMAGNETIC COMPATIBILITY. He was a guest editor a special issue on "Advanced Numerical Techniques in Electromagnetics" of the IEEE TRANSACTIONS ON ANTENNAS AND PROPAGATION (March 1997). He has been an invited convener at URSI General Assemblies for special sessions on field and waves (1996) and electromagnetic metrology and computational electromagnetics (1999). He organized the special session on electromagnetic compatibility at the 1998 URSI International Symposium on electromagnetic theory. Since 1999, he has been the general chairperson of the Biennial International Conference on Electromagnetics in Advanced Applications (ICEAA), Turin, Italy.